© 2018. Published by The Company of Biologists Ltd | Journal of Experimental Biology (2018) 221, jeb174474. doi:10.1242/jeb.174474

RESEARCH ARTICLE

Are the surface areas of the gills and body involved with changing metabolic scaling with temperature?

Ge Li[1,2,*], Xiao Lv[1,*], Jing Zhou[3], Cong Shen[1], Danyang Xia[1], Hang Xie[4] and Yiping Luo[1,‡]

ABSTRACT

The metabolic-level boundaries (MLB) hypothesis proposes that metabolic level mediates the relative influence of surface area (SA)- versus volume-related metabolic processes on the body-mass scaling of metabolic rate in organisms. The variation in the scaling of SA may affect how metabolic level affects the metabolic scaling exponent. This study aimed to determine the influence of increasing metabolic level at a higher temperature on the metabolic scaling exponent of the goldfish and determine the link between metabolic scaling exponents and SA parameters of both gills and body. The SA of gills and body and the resting metabolic rate (RMR) of the goldfish were assessed at 15°C and 25°C, and their mass scaling exponents were analyzed. The results showed a significantly higher RMR, with a lower scaling exponent, in the goldfish at a higher temperature. The SA of the gills and the total SA of the fish (TSA) were reduced with the increasing temperature. The scaling exponent of RMR (b_{RMR}) tended to be close to that of the TSA at a higher temperature. This suggests that temperature positively affects metabolic level but negatively affects b_{RMR}. The findings support the MLB hypothesis. The lower scaling exponent at a higher temperature can be alternatively explained as follows: the higher viscosity of cold water impedes respiratory ventilation and oxygen uptake and reduces metabolic rate more in smaller individuals than in larger individuals at lower temperature, thus resulting in a negative association between temperature and b_{RMR}.

KEY WORDS: Fish, Body size, Respiration, Allometric

INTRODUCTION

The metabolic rate (MR) of animals is related to body mass (M_b). MR scales with M_b according to the power equation $MR=aM^b$, where a is a constant and b is the scaling exponent. This relationship has attracted many researchers over the past century. Many important hypotheses regarding the scaling of MR have been proposed (Glazier, 2014a), e.g. the organ size hypothesis (Itazawa and Oikawa, 1983; Oikawa et al., 1992), the fractal resource distribution network hypothesis (West et al., 1997; Brown et al., 2004), the surface area (SA) hypothesis (Rubner, 1883; Okie, 2013) and the metabolic-level boundaries (MLB) hypothesis (Glazier, 2005, 2008, 2009, 2010).

The SA hypothesis assumes that metabolic scaling is strongly influenced by the transport of materials through external exchange surfaces, such as skin, lungs and gills (Rubner, 1883; Okie, 2013), and that MR is proportional to the surface area of an isomorphically growing organism, and it predicts that the intraspecific b-value (b_{RMR}) for the resting metabolic rate (RMR) is equal to 2/3 (Rubner, 1883). According to the Euclidean surface area predictions, the b-value (b_{BSA}) of body surface area (BSA) can be predicted from the M_b–body length (L) scaling exponent b_L. When organisms grow isomorphically throughout ontogeny, b_L is equal to 3 and b_{BSA} could be 2/3. However, when the growing mode of an organism is anisomorphic (elongated, flatted or thickened), b_{BSA} could be different than 2/3, which causes varying b_{RMR} among species (Okie, 2013; Hirst et al., 2014).

The MLB hypothesis proposes that metabolic level, the vertical elevation of a metabolic scaling relationship, mediates the relative influence of SA- versus volume-related metabolic processes on the body-mass scaling of metabolic rate in organisms (Glazier, 2005, 2008, 2009, 2010, 2014b). When the metabolic level is high, metabolic scaling should be chiefly influenced by fluxes of resources, wastes and/or heat across surfaces (scaling as $M_b^{2/3}$). However, when the metabolic level is low and amply met by surface-dependent processes, metabolic scaling should be more related to the energy demand required to sustain the tissues, which is directly proportional to tissue mass or volume (scaling as M_b^1) (Glazier, 2008). Therefore, organisms with higher RMR have a lower intraspecific metabolic scaling exponent, that is, b_{RMR} is negatively correlated with the metabolic level (Glazier, 2005, 2008, 2009, 2010). Aside from the effect of the metabolic level on b_{RMR}, factors influencing the relative effects of a surface- or volume-related process should also affect metabolic scaling (Glazier, 2014b), which has been supported by our recent work, which showed that a negative correlation exists between SA of red blood cells and intraspecific b_{RMR} among several fish species (Luo et al., 2015). It can be hypothesized that the variation in SA and its scaling may affect how metabolic level affects b_{RMR}.

In water-breathing fish, the gill is mainly responsible for the transport of oxygen and metabolic wastes (Perry et al., 2009). Studies have compared the scaling exponent (b_{GSA}) of the gill surface area (GSA) with b_{RMR} in several species of fish (Oikawa and Itazawa, 1985; Oikawa et al., 1999). However, whether GSA limits b_{RMR} remains unclear, as GSA is more related to activity metabolism but not resting metabolism (Hughes, 1984; Oikawa and Itazawa, 1985; Oikawa et al., 1999; Killen et al., 2016). Unfortunately, those previous data of b_{GSA} were not determined together with b_{RMR} in the same specimen of an experiment. As the b_{GSA} and b_{RMR} of a species may vary depending on multiple factors (e.g. temperature, dissolved oxygen, predation regime and habitat)

[1]Key Laboratory of Freshwater Fish Reproduction and Development, Ministry of Education, School of Life Sciences, Southwest University, Chongqing 400715, China. [2]Wudu Bayi High School, Wudu, Longnan, Gansu 746000, China. [3]Department of Clinical Medicine, Chongqing Medical and Pharmaceutical College, Chongqing 401331, China. [4]Luzhou Agricultural Bureau, National Nature Reserve of Rare and Endemic Fish in the Upper Yangtze River for Luzhou Workstation, Luzhou, Sichuan 646009, China.
*These authors contributed equally to this work

‡Author for correspondence (luoguo@swu.edu.cn)

G.L., 0000-0003-2048-1158; J.Z., 0000-0002-2845-7112; Y.L., 0000-0003-3312-6403

Received 21 November 2017; Accepted 13 March 2018

(Ohlberger et al., 2012; Luo and Wang, 2012; Glazier et al., 2011; Mcfeeters et al., 2011; Glazier and Paul, 2017), a comparison of the b_{GSA} and b_{RMR} of the same fish species in one experiment seems to be necessary.

In addition to the gills, the skin of fish may play an exchange role (Hughes and Al-Kadhomiy, 1988; Glover et al., 2013). Approximately 10–30% of resting oxygen uptake is via the skin of adult water-breathing fish (Kirsch and Nonnotte, 1977; Steffensen et al., 1981; Feder and Burggren, 1985; Takeda, 1990). It can be assumed that the exchange capacity of the fish body may be linked to its total surface area (TSA), including not only GSA, but also body surface area (BSA). In the larvae of Atlantic salmon (*Salmo salar*), the scaling exponent of TSA (b_{TSA}, 0.95) was virtually identical to b_{RMR} (0.94) (Wells and Pinder, 1996a,b), implying a close link between the two parameters. Therefore, according to the MLB hypothesis, it can be hypothesized that the increase in metabolic level may result in a reduction of b_{RMR} to values tending to be close to b_{TSA}.

Temperature is one important ecological factor influencing the metabolic level of fish (Jobling, 1994; Clarke and Johnston, 1999; Peck et al., 2003, 2005; Ohlberger et al., 2012; Luo and Wang, 2012). The metabolic level of fish increases as temperature increases, which reduces the intraspecific metabolic scaling exponent, as b_{RMR} is negatively correlated with metabolic level (Glazier, 2005, 2008, 2009, 2010). The negative effects of higher temperatures on b_{RMR} have been observed in many fish species (Xie and Sun, 1990; Killen et al., 2010; Luo and Wang, 2012). However, the increase in temperature may change the exchange SA of fish. For example, the functional respiratory area of gills may be enlarged by thermal plastic remodeling in the goldfish [*Carassius auratus* (Linnaeus 1758)] (Sollid et al., 2005; Sollid and Nilsson, 2006). Thus, the potential surface constraints of the gill exchange surface can be changed by temperature. The determination of respiratory SA, accompanied with the metabolic level of fish, may supply strong evidence for the effect of temperature on b_{RMR}.

In the present study, RMR and the exchange SA parameters, including BSA, GSA and TSA, of the goldfish were assessed at two temperatures, 15°C and 25°C. Then, the scaling exponents of those parameters were analyzed. Our earlier studies have suggested that previous theories can only partially explain the scaling exponent of RMR of the goldfish (Huang et al., 2013; Li et al., 2016). It remains unclear which exchange surface constricts the metabolic scaling exponent of the goldfish and how temperature affects its metabolic scaling. This study aimed to determine the influence of increasing the metabolic level at a higher temperature on the metabolic scaling of the goldfish and determine the link between metabolic scaling exponents and SA parameters of both the gills and the body.

MATERIALS AND METHODS

Goldfish (body mass ranging from 4 to 250 g) were obtained from local fisheries in Chongqing, China. All handling and treatment was conducted in accordance with the ethical requirements for animal care of the School of Life Sciences of Southwest University, China, and the requirements of environment and housing facilities for laboratory animals in China (Gb/T14925-2001). The fish were randomly divided into two groups and were acclimated in a rearing system at 15.0±0.2°C and 25.0±0.2°C, respectively, for 4 weeks. During acclimation, the dissolved oxygen was kept higher than 90% saturated concentration, ammonia-N was kept below 0.01 mg l^{-1}, and the photoperiod was 12 h:12 h light:dark. The fish were fed once at 18:00 h daily, with commercial diets at a ration of 1% of M_b. The chemical composition of the diet was 12.5% moisture, 33.0% protein, 3.0% fat and 10.0% digestible carbohydrate. At the end of the acclimation period, fish were fasted for 48 h and individually placed into the chambers of a continuous flow respirometer overnight. Then, the oxygen consumption rate was measured as described by Wang et al. (2012). Chamber sizes (0.13, 0.52, 0.86 and 1.20 liters) were dependent on the M_b of the experimental individual. Up to six individuals were subjected to measurements at the same time, and one chamber without fish was used to control the background oxygen consumption. The oxygen consumption rate of each individual was measured hourly for 6 h, and the mean value of the lowest two measurements was used as the RMR for that individual. The individual oxygen consumption rate ($\dot{M}_{O_2}$; mg O_2 h^{-1}) was calculated by the following formula:

$$\dot{M}_{O_2} = \Delta C_{DO} \times v, \quad (1)$$

where ΔC_{DO} is the difference in the dissolved oxygen concentration (mg O_2 l^{-1}) between the outlets of an experimental chamber and the control chamber, and v is the water flow rate through the chamber (l h^{-1}). The dissolved oxygen concentration was measured at the outlet of the chamber using an oxygen meter (HQ30, Hach Company, Loveland CO, USA). The water flow rate was determined by collecting the outflow water into a beaker over a given period of time. The water flow rate was adjusted to ensure that the oxygen concentration in the outlet water was higher than 7 mg l^{-1} to avoid physiological stress (Zhang et al., 2014).

Once the determination of RMR was finished, the fish were killed by an overdose of anesthetic. M_b was weighed to the nearest 0.1 g, and L was measured to the nearest 0.1 cm. For the fish at 25°C, M_b ranged from 4.24 to 299.6 g (mean±s.d.=63.32±64.98 g) and L ranged from 7.13 to 23.78 g (mean±s.d.=14.37±5.31 cm). For the fish at 15°C, M_b ranged from 4.42 to 223.2 g (mean±s.d.=68.32±68.99 g) and L ranged from 7.47 to 24.03 g (mean±s.d.=15.01±5.38 cm). Then, all fins were dissected from the body of each individual, and a piece of plastic paper was stuck to the fish body, equal in shape and size, to fix body regions (Jaworski and Holm, 1992; Tucker et al., 2002; O'Shea et al., 2006). The fins and the plastic paper were laid out and photographed to measure the SA using the computer-linked image-analysis program Image-Pro Plus 6.0 (Media Cybernetics, Rockville, MD, USA). Next, the gill mass (M_g) was measured, and the first four gill arches were dissected from the left gill of the fish and put into Bouin's fluid. The gills were kept in the fixative for 2 days before transfer to 70% alcohol just before measuring GSA. GSA was calculated using a standardized gill morphology assessment (Hughes, 1966, 1984) with a microscope (Aigo Digital Technology Co., Beijing, China). The number of filaments on each gill arch was counted. Then, each arch was divided into six equal parts, and one middle filament of each part was chosen to measure the filament length and the secondary lamellae frequency on one side of the filament. Lastly, the bilateral areas of the secondary lamellas of the filaments from the second arch were determined as an averaged lamellae area. Total filament number (FN), total length of all gill filaments (TFL, mm), mean filament length (FL, mm), mean lamellae frequency (LF, mm^{-1}) and mean lamella area (LA, mm^2) were obtained. The following formula was employed to calculate the GSA (mm^2) of an individual: GSA=4×TFL×LF×LA. The final numbers of fish specimens were 30 for 25°C and 28 for 15°C.

The data were calculated using Microsoft Excel 2003 (Microsoft Corporation, Redmond, WA, USA), and statistical analysis was conducted using SAS (PROC MODEL, SAS v.9.4; SAS Institute, Cary, NC, USA). The original data were used for size allometric

Journal of Experimental Biology (2018) 221, jeb174474. doi:10.1242/jeb.174474

analysis using nonlinear regression and were fitted to three sets of four models, involving two straight lines and two power functions: assumed additive, normal, homoscedastic error or additive, normal, heteroscedastic error, and multiplicative, lognormal, heteroscedastic error (Lolli et al., 2017; Packard, 2017). Ordinary least squares regression was used for regression procedures. The SAS programming code used in the present study is modified from the code of Packard (2017) and is available online (see Script 1). Parameters (a, b, c, d and $y0$) were estimated based on the Marquardt procedure. The treatments ware set as 0 for fish at 15°C and 1 for those at 25°C. For each model, the effect of temperature on each variable was tested by the coefficient of the temperature term (c), and the effect of temperature on scaling exponent was tested by the coefficient of the interaction term (d) (Script 1). If the value for d was not significant, then the model with no interaction term was used for analysis. If the value for c was not significant, then the model with no temperature term was used for analysis. Akaike's information criterion (AIC) was used to examine the quality of models (Burnham et al., 2011; Lolli et al., 2017; Packard, 2017). The model with the smallest AIC value was referred to as the best model and the AIC difference (ΔAIC) from the best model was used to rank the models (Burnham et al., 2011; Lolli et al., 2017; Packard, 2017). Regression parameters of scaling slopes were reported with 95% confidence intervals (CI) in graphs. Each scaling slope was compared with 2/3 using 95% CI. P-values less than 0.05 were considered statistically significant.

RESULTS

The regressions between M_b and most parameters including RMR, TSA, GSA, BSA, TFL, FN, LF and LA had the lowest ΔAIC values using models with lognormal, heteroscedastic error (model 9, 12 in Table S1). Most of those relationships were described with the best quality by the power function (with intercept) with lognormal, heteroscedastic error (model 12). The power functions (no intercept) with lognormal, heteroscedastic error (model 9) also worked satisfactorily, with low ΔAIC values (mostly lower than 2) for most relationships and with the best quality for the relationship between RMR and M_b. The regressions between GSA and M_g also had lognormal, heteroscedastic error and could be described by the power functions and straight lines with (or without) intercept satisfactorily. Thus, power functions with no intercept (model 9) were adopted and displayed in log–log graphs for ease of comparison with traditionally reported scaling functions.

RMR of the goldfish was higher at 25°C than at 15°C (c=0.994, P<0.0001) and the b_{RMR} at 15°C (0.898) was significantly larger than that at 25°C (0.815; Fig. 1), as demonstrated by the significant interaction between temperature and M_b (d=−0.0826, P=0.0418; model 9 in Table S1).

TSA of the goldfish scaled with M_b by a b_{TSA} of 0.837 at 25°C, larger than that at 15°C (0.789; Fig. 2), as demonstrated by the significant d value (d=0.0475, P=0.0332; model 9 in Table S1). b_{GSA} and b_{BSA} were not significantly different between temperatures, and the common values (b_{GSA}: 0.889; b_{BSA}: 0.673) were used for both temperatures. b_{GSA} and b_{TSA} were significantly larger than 2/3 at both temperatures. At 25°C, b_{RMR} was different to both b_{BSA} and b_{GSA}, but not to b_{TSA}, whereas at 15°C, b_{RMR} was different to both b_{BSA} and b_{TSA}, but not to b_{GSA} (Figs 1 and 2). The results showed the negative effects of temperature on both TSA and GSA, as demonstrated by the small but significant c values (c=−0.244, P=0.0044 for TSA; c=−0.101, P=0.0286 for GSA) (model 9 in Table S1). BSA showed no significant difference between temperatures.

GSA scaled with M_g by the common b value of 1.019 at both temperatures (Fig. 3; model 9 in Table S1). TFL, FL and LF scaled with M_b and showed no significant differences in both scaling exponents and intercepts between temperatures (Table S1). FN and

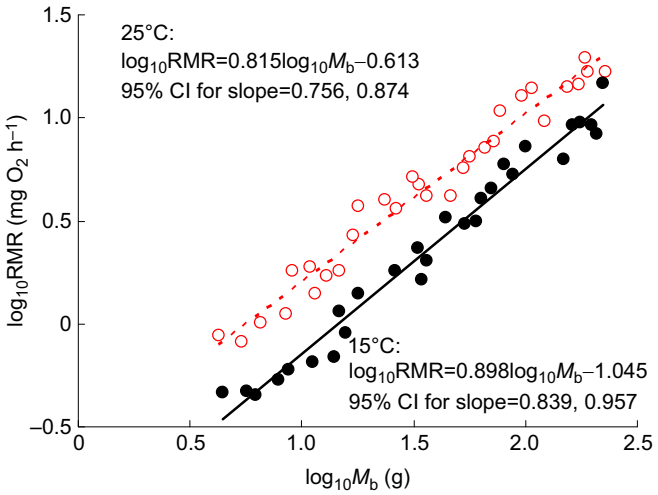

Fig. 1. The relationship between resting metabolic rate (RMR) and body mass (M_b) of the goldfish. Two-parameter power function with lognormal, heteroscedastic error models fitted to untransformed data. n=30 for 25°C and n=28 for 15°C. Red open circles and red dashed line: 25°C; black filled circles and black solid line: 15°C.

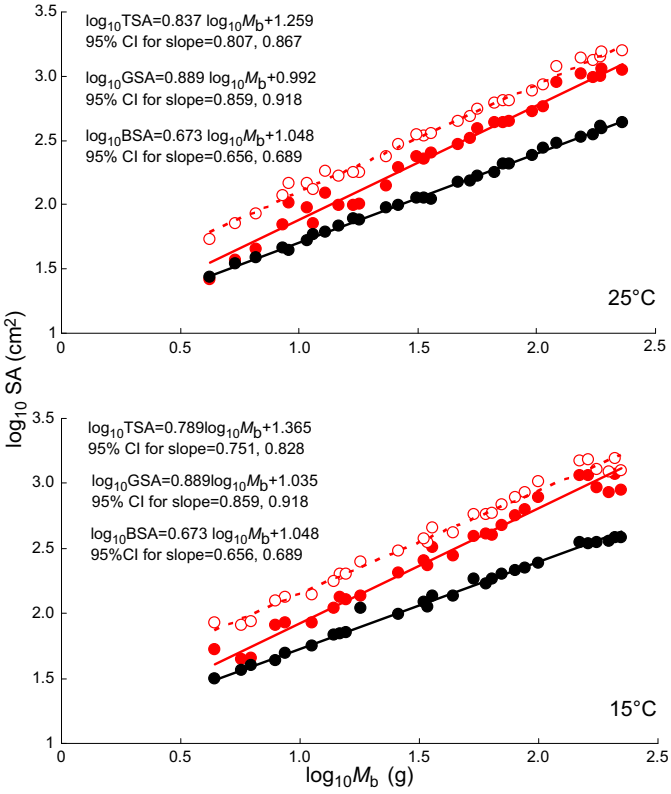

Fig. 2. The relationship between surface area (SA) and body mass (M_b) of the goldfish at 25°C and 15°C. Two-parameter power function with lognormal, heteroscedastic error models fitted to untransformed data. n=30 for 25°C and n=28 for 15°C. Red open circles and red dashed line: total surface area (TSA); red filled circles and red solid line: gill surface area (GSA); black filled circles and black solid line: body surface area (BSA).

Journal of Experimental Biology (2018) 221, jeb174474. doi:10.1242/jeb.174474

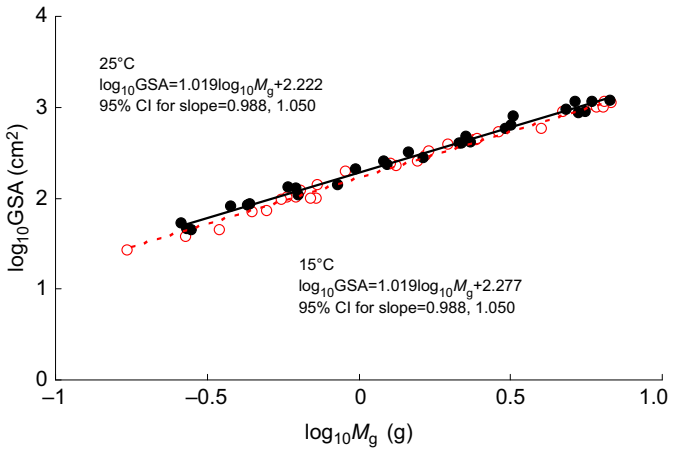

Fig. 3. The relationship between gill surface area (GSA) and gill mass (M_g) of the goldfish. Two-parameter power function with lognormal, heteroscedastic error models fitted to untransformed data. n=30 for 25°C and n=28 for 15°C. Red open circles and red dashed line: 25°C; black filled circles and black solid line: 15°C.

LA also scaled with M_b by common scaling exponents at both temperatures. However, the significant c values for FN (−0.0438) and LA (−0.0863) showed negative effects of temperature (model 9 in Table S1).

DISCUSSION

Our study presented a positive association between temperature and RMR, but a negative association between temperature and b_{RMR} in the goldfish, which can be explained by the MLB hypothesis that the increase in metabolic level intensifies the relative importance of surface area processes on fluxes of resources, wastes and/or heat (Glazier, 2005, 2008, 2009, 2010), and/or by changes in relative exchange SA (Luo et al., 2015). The negative effect of metabolic level on b_{RMR} in our study supports the MLB hypothesis. In addition, the results showed a small but significant reduction in the values of TSA and GSA of the goldfish from 15°C to 25°C, which suggests that the plasticity in exchange surfaces at the individual level may also contribute to the reduced b_{RMR} at the higher temperature. Whether the exchange surfaces at the cellular level change with temperature needs to be further studied.

The oxygen uptake of fish occurs via its whole surface, including not only the gills but also the skin (Feder and Burggren, 1985; Glover et al., 2013). Actually, a considerable proportion of oxygen transfers occur via the fish body surface, e.g. 12% in the carp (*Cyprinus carpio*), 13% in the trout (*Salmo gairdnerii*), 23% in the tench (*Tinca tinca*) and 27% in the plaice (*Pleuronectes platessa*) (Kirsch and Nonnotte, 1977; Steffensen et al., 1981; Takeda, 1990). The present results showed that the b_{RMR} was larger than the b_{TSA} at 15°C, and the two tended to be equal at 25°C, which agrees with our prediction. It can be explained, according to the MLB hypothesis (Glazier, 2005, 2008, 2009, 2010; Hirst et al., 2014), that the low metabolic demand and thus the weak constraints of TSA allow a larger b_{RMR} at a lower temperature, whereas at a higher temperature, the enhanced constraints of TSA on RMR result in a lower b_{RMR}, tending to be close to b_{TSA}. An alternative explanation for the present results can be deduced according to the viscosity hypothesis proposed by Verberk and Atkinson (2013). The viscosity of water increases with decreasing temperature (Jumars et al., 1993; Von Herbing, 2002). According to the equation in Jumars et al. (1993), the viscosity of freshwater is 0.89×10^{6} m^2 s^{-1} at 25°C and 1.14×10^{6} m^2 s^{-1} at 15°C, suggesting an approximately 28% increase in the viscosity of the water cooling down from 25°C to 15°C in our study. The higher viscosity of cold water results in thicker boundary layers and larger drag, and thus may impede respiratory ventilation and oxygen uptake of aquatic organisms (Verberk and Atkinson, 2013). For very small organisms (<1 mg), oxygen uptake can be met by diffusion rather than convection of water, and the effect of water viscosity on oxygen uptake is not important; however, for organisms heavier than 1 mg, oxygen uptake switches to be convection dependent and is affected by water viscosity more seriously in smaller individuals because of smaller Reynolds number (Makarieva et al., 2008; Verberk and Atkinson, 2013). Therefore, within the organisms beyond the critical size of 1 mg, smaller individuals may exhibit a greater depression of MR than that of larger individuals at lower temperature, thus resulting in a negative association between temperature and b_{RMR}.

Many previous theories have attributed metabolic scaling to the limits of the exchange SA of organisms, which was assumed to scale by $M_b^{2/3}$ (Rubner, 1883; Okie, 2013). In the present study, the value of b_{BSA} of the goldfish (0.673) was not significantly different to 2/3, but the value of b_{GSA} (0.889) was larger than 2/3, independent of temperature. Greater than 2/3 scaling in respiratory SA is common, as the gill has high fractal dimensions (Okie, 2013; Weibel et al., 1991), e.g. 0.997 in three tunny species (Muir and Hughes, 1969), 0.85 in Atlantic mackerel *Scomber scombrus* (Hughes and Gray, 1972), 0.900 in *Oncorhynchus mykiss* (Jager and Dekkers, 1975), 0.794 in *C. carpio* (Oikawa and Itazawa, 1985), 0.813 in *P. major* (Oikawa et al., 1999) and 0.768 in *Sander lucioperca* (Satora and Wegner, 2012). In addition, the TSA of the goldfish also scaled with body mass by exponents larger than 2/3 at both temperatures. Similarly, previous studies have proposed that the scaling exponent of SA may be different to 2/3 (Glazier, 2010, 2014b). Those results suggest that the exchange SA may scale with body mass by different exponents, depending on the objective SA, and that the presupposed scaling value of 2/3 for the SA needs to be modified.

Our results showed a small, negative change in the GSA of the goldfish from 15°C to 25°C, different to a previous report (Sollid et al., 2005), which could be due to the relative warmer temperature range in our study. The remarkable increase of the GSA of the goldfish occurred within a lower temperature range (from 7.5°C to 15°C), and no further obvious changes were observed above 15°C (Sollid et al., 2005). The ontogenetic changes in GSA can be attributed to changes in different gill constituent variables depending on species, such as an increase in secondary lamellae area (Muir and Hughes, 1969; Mazon et al., 1998; Hartl et al., 2000) and an increase in filament length or lamellae frequency (Severi et al., 1997; Mazon et al., 1998; Timmerman and Chapman, 2004; Karakatsouli et al., 2006). LA and FL scaled with M_b of the goldfish by exponents larger than that of LF, which suggests that the increase in GSA with M_b is mainly attributed to the increase in LA and FL. In addition, GSA scaled isometrically with M_g (scaling exponent: 1.019) at both temperatures. Compared with GSA, M_g is a variable that can be determined more easily. Therefore, it suggests a potential method to estimate mass scaling of GSA conveniently by determining the mass scaling of M_g.

In conclusion, the present study supplied comparable data of several SA parameters and RMR, as well as the mass scaling exponents of the goldfish under different temperatures. The results verified the negative effect of metabolic level on b_{RMR} and showed that the increase in metabolic level with temperature resulted in a reduction of b_{RMR} to values tending to be close to b_{TSA}, which supports the MLB hypothesis. An alternative explanation is that the

higher viscosity of cold water impedes respiratory ventilation and oxygen uptake and reduces MR more in smaller individuals than in larger individuals at lower temperature, thus resulting in a negative association between temperature and b_{RMR}.

Acknowledgements
We thank Mr Bo Zhang for his help in fish collection. We sincerely thank the anonymous reviewers for their helpful suggestions and comments.

Competing interests
The authors declare no competing or financial interests.

Author contributions
Conceptualization: Y.L.; Methodology: G.L., X.L., J.Z., H.X., Y.L.; Software: G.L., X.L., Y.L.; Validation: G.L., C.S., D.X., Y.L.; Formal analysis: X.L., J.Z., C.S., D.X., H.X.; Investigation: G.L., X.L., J.Z., H.X., Y.L.; Resources: H.X., Y.L.; Data curation: X.L., Y.L.; Writing - original draft: G.L.; Writing - review & editing: X.L., J.Z., C.S., D.X., Y.L.; Supervision: Y.L.; Project administration: Y.L.; Funding acquisition: Y.L.

Funding
This work was supported by the National Natural Science Foundation of China (no. 31672287).

Data availability
Data for this study have been deposited in figshare: https://doi.org/10.6084/m9.figshare.5844930.v1

Supplementary information
Supplementary information available online at
http://jeb.biologists.org/lookup/doi/10.1242/jeb.174474.supplemental

References

Brown, J. H., Gillooly, J. F., Allen, A. P., Savage, V. M. and West, G. B. (2004). Toward a metabolic theory of ecology. *Ecology* **85**, 1771-1789.
Burnham, K. P., Anderson, D. R. and Huyvaert, K. P. (2011). AIC model selection and multimodel inference in behavioral ecology: some background, observations, and comparisons. *Behav. Ecol. Sociobiol.* **65**, 415-415.
Clarke, A. and Johnston, N. M. (1999). Scaling of metabolic rate with body mass and temperature in teleost fish. *J. Anim. Ecol.* **68**, 893-905.
Feder, M. E. and Burggren, W. W. (1985). Cutaneous gas exchange in vertebrates: design, patterns, control and implications. *Biol. Rev.* **60**, 1-45.
Glazier, D. S. (2005). Beyond the '3/4-power law': variation in the intra- and interspecific scaling of metabolic rate in animals. *Biol. Rev.* **80**, 611-662.
Glazier, D. S. (2008). Effects of metabolic level on the body size scaling of metabolic rate in birds and mammals. *Proc. R. Soc. B* **275**, 1405-1410.
Glazier, D. S. (2009). Activity affects intraspecific body-size scaling of metabolic rate in ectothermic animals. *J. Comp. Physiol. B* **179**, 821-828.
Glazier, D. S. (2010). A unifying explanation for diverse metabolic scaling in animals and plants. *Biol. Rev.* **85**, 111-138.
Glazier, D. S. (2014a). Metabolic scaling in complex living systems. *Systems* **2**, 451-540.
Glazier, D. S. (2014b). Scaling of metabolic scaling within physical limits. *Systems* **2**, 425-450.
Glazier, D. S. and Paul, D. A. (2017). Ecology of ontogenetic body-mass scaling of gill surface area in a freshwater crustacean. *J. Exp. Biol.* **220**, 2120-2127.
Glazier, D. S., Butler, E. M., Lombardi, S. A., Deptola, T. J., Reese, A. J. and Satterthwaite, E. V. (2011). Ecological effects on metabolic scaling: amphipod responses to fish predators in freshwater springs. *Ecol. Monogr.* **81**, 599-618.
Glover, C. N., Bucking, C. and Wood, C. M. (2013). The skin of fish as a transport epithelium: a review. *J. Comp. Physiol. B* **183**, 877-891.
Hartl, M. G. J., Hutchinson, S., Hawkins, L. E. and Eledjam, M. (2000). The biometry of gills of 0-group European flounder. *J. Fish Biol.* **57**, 1037-1046.
Hirst, A. G., Glazier, D. S. and Atkinson, D. (2014). Body shape shifting during growth permits tests that distinguish between competing geometric theories of metabolic scaling. *Ecol. Lett.* **17**, 1274-1281.
Huang, Q., Zhang, Y., Liu, S., Wang, W. and Luo, Y. (2013). Intraspecific scaling of the resting and maximum metabolic rates of the crucian carp (*Carassius auratus*). *PLoS ONE* **8**, e82837.
Hughes, G. M. (1966). The dimensions of fish gills in relation to their function. *J. Exp. Biol.* **45**, 177-195.
Hughes, G. M. (1984). Scaling of respiratory areas in relation to oxygen consumption of vertebrates. *Cell. Mol. Life Sci.* **40**, 519-524.
Hughes, G. M. and Al-Kadhomiy, N. K. (1988). Changes in scaling of respiratory systems during the development of fishes. *J. Mar. Biol. Assoc. UK* **68**, 489-498.
Hughes, G. M. and Gray, I. E. (1972). Dimensions and ultrastructure of toadfish gills. *Biol. Bull.* **143**, 150-161.
Itazawa, Y. and Oikawa, S. (1983). Metabolic rates in excised tissues of carp. *Experientia* **39**, 160-161.
Jager, S. D. and Dekkers, W. J. (1975). Relations between gill structure and activity in fish. *Neth. J. Zool.* **25**, 276-308.
Jaworski, A. and Holm, J. C. (1992). Distribution and structure of the population of sea lice, *Lepeophtheirus salmonis* Krøyer, on Atlantic salmon, *Salmo salar* L. under typical rearing conditions. *Aquac. Res.* **23**, 577-589.
Jobling, M. (1994). *Fish Bioenergetics.* London: Chapman and Hall.
Jumars, P. A., Dewing, J. W., Hill, P. S., Karpboss, L., Yager, P. L. and Dade, W. B. (1993). Physical constraints on marine osmotrophy in an optimal foraging context. *Mar. Microbiol. Food Webs* **7**, 121-159.
Karakatsouli, N., Tarnaris, K., Balaskas, C. and Papoutsoglou, S. E. (2006). Gill area and dimensions of gilthead sea bream *Sparus aurata* L. *J. Fish Biol.* **69**, 291-299.
Killen, S. S., Atkinson, D. and Glazier, D. S. (2010). The intraspecific scaling of metabolic rate with body mass in fishes depends on lifestyle and temperature. *Ecol. Lett.* **13**, 184-193.
Killen, S. S., Glazier, D. S., Rezende, E. L., Clark, T. D., Atkinson, D., Willener, A. S. T. and Halsey, L. G. (2016). Ecological influences and morphological correlates of resting and maximal metabolic rates across teleost fish species. *Am. Nat.* **187**, 592-606.
Kirsch, R. and Nonnotte, G. (1977). Cutaneous respiration in three freshwater teleosts. *Resp. Physiol.* **29**, 339-354.
Li, G., Xie, H., He, D. and Luo, Y. (2016). Effects of body chemical components on the allometric scaling of the resting metabolic rate in four species of cyprinids. *Fish Physiol. Biochem.* **42**, 295-301.
Lolli, L., Batterham, A. M., Kratochvíl, L., Flegr, J., Weston, K. L. and Atkinson, G. (2017). A comprehensive allometric analysis of 2nd digit length to 4th digit length in humans. *Proc. R. Soc. B* **284**, 20170356.
Luo, Y. P. and Wang, Q. Q. (2012). Effects of body mass and temperature on routine metabolic rate of juvenile largemouth bronze gudgeon *Coreius guichenoti*. *J. Fish Biol.* **80**, 842-851.
Luo, Y., He, D., Li, G., Xie, H., Zhang, Y. and Huang, Q. (2015). Intraspecific metabolic scaling exponent depends on red blood cell size in fishes. *J. Exp. Biol.* **218**, 1496-1503.
Makarieva, A. M., Gorshkov, V. G., Li, B.-L., Chown, S. L., Reich, P. B. and Gavrilov, V. M. (2008). Mean mass-specific metabolic rates are strikingly similar across life's major domains: evidence for life's metabolic optimum. *Proc. Natl. Acad. Sci. USA* **105**, 16994-16999.
Mazon, A. D. F., Fernandes, M. N., Nolasco, M. A. and Severi, W. (1998). Functional morphology of gills and respiratory area of two active rheophilic fish species, *Plagioscion squamosissimus* and *Prochilodus scrofa*. *J. Fish Biol.* **52**, 50-61.
Mcfeeters, B. J., Xenopoulos, M. A., Spooner, D. E., Wagner, N. D. and Frost, P. C. (2011). Intraspecific mass-scaling of field metabolic rates of a freshwater crayfish varies with stream land cover. *Ecosphere* **2**, art13.
Muir, B. S. and Hughes, G. M. (1969). Gill dimensions for three species of tunny. *J. Exp. Biol.* **51**, 271-285.
Ohlberger, J., Mehner, T., Staaks, G. and Hölker, F. (2012). Intraspecific temperature dependence of the scaling of metabolic rate with body mass in fishes and its ecological implications. *Oikos* **121**, 245-251.
Oikawa, S. and Itazawa, Y. (1985). Gill and body surface areas of the carp in relation to body mass, with special reference to the metabolism-size relationship. *J. Exp. Biol.* **117**, 1-14.
Oikawa, S., Takemori, M. and Itazawa, Y. (1992). Relative growth of organs and parts of a marine teleost, the porgy, *Pagrus major*, with special reference to metabolism size relationships. *Jpn. J. Ichthyol.* **39**, 243-249.
Oikawa, S., Hirata, M., Kita, J. and Itazawa, Y. (1999). Ontogeny of respiratory area of a marine teleost, porgy, *Pagrus major*. *Ichthyol. Res.* **46**, 233-244.
Okie, J. G. (2013). General models for the spectra of surface area scaling strategies of cells and organisms: fractality, geometric dissimilitude, and internalization. *Am. Nat.* **181**, 421-439.
O'Shea, B., Mordue-Luntz, A. J., Fryer, R. J., Pert, C. C. and Bricknell, I. R. (2006). Determination of the surface area of a fish. *J. Fish Dis.* **29**, 437-440.
Packard, G. C. (2017). Is complex allometry in field metabolic rates of mammals a statistical artifact? *Comp. Biochem. Physiol. A* **203**, 322-327.
Peck, M. A., Buckley, L. J. and Bengtson, D. A. (2003). Energy losses due to routine and feeding metabolism in young-of-the-year juvenile Atlantic cod (*Gadus morhua*). *Can. J. Fish. Aquat. Sci.* **60**, 929-937.
Peck, M. A., Buckley, L. J. and Bengtson, D. A. (2005). Effects of temperature, body size and feeding on rates of metabolism in young-of-the-year haddock. *J. Fish Biol.* **66**, 911-923.
Perry, S. F., Esbaugh, A., Braun, M. and Gilmour, K. M. (2009). Gas transport and gill function in water-breathing fish. In *Cardio-Respiratory Control in Vertebrates* (ed. M. Glass and S. Wood), pp. 5-42. Berlin, Heidelberg: Springer.
Rubner, M. (1883). Über den Einfluss der Körpergrösse auf Stoff- und Kraftwechsel. *Zeit. Biol.* **19**, 535-562.
Satora, L. and Wegner, N. C. (2012). Reexamination of the Byczkowska-Smyk gill surface area data for European teleosts, with new measurements on the pikeperch, *Sander lucioperca*. *Rev. Fish Biol. Fisher.* **22**, 1-9.

Severi, W., Rantin, F. T. and Fernandes, M. N. (1997). Respiratory gill surface of the serrasalmid fish, *Piaractus mesopotamicus*. *J. Fish Biol.* **50**, 127-136.
Sollid, J. and Nilsson, G. E. (2006). Plasticity of respiratory structures-adaptive remodeling of fish gills induced by ambient oxygen and temperature. *Resp. Physiol. Neurobi.* **154**, 241-251.
Sollid, J., Weber, R. E. and Nilsson, G. E. (2005). Temperature alters the respiratory surface area of crucian carp *Carassius carassius* and goldfish *Carassius auratus*. *J. Exp. Biol.* **208**, 1109-1116.
Steffensen, J. F., Lomholt, J. P. and Johansen, K. (1981). The relative importance of skin oxygen uptake in the naturally buried plaice, *Pleuronectes platessa*, exposed to graded hypoxia. *Respir. Physiol.* **44**, 269-275.
Takeda, T. (1990). Cutaneous and gill O_2 uptake in the carp, *Cyprinus carpio*, as a function of metabolic rate. *Comp. Biochem. Physiol. A* **95**, 425-427.
Timmerman, C. M. and Chapman, L. J. (2004). Hypoxia and interdemic variation in *Poecilia latipinna*. *J. Fish Biol.* **65**, 635-650.
Tucker, C. S., Sommerville, C. and Wootten, R. (2002). Does size really matter? Effects of fish surface area on the settlement and initial survival of *Lepeophtheirus salmonis*, an ectoparasite of Atlantic salmon *Salmo salar*. *Dis. Aquat. Org.* **49**, 145-152.
Verberk, W. C. and Atkinson, D. (2013). Why polar gigantism and palaeozoic gigantism are not equivalent: effects of oxygen and temperature on the body size of ectotherms. *Funct. Ecol.* **27**, 1275-1285.
Von Herbing, I. H. (2002). Effects of temperature on larval fish swimming performance: the importance of physics to physiology. *J. Fish Biol.* **61**, 865-887.
Wang, Q., Wang, W., Huang, Q., Zhang, Y. and Luo, Y. (2012). Effect of meal size on the specific dynamic action of the juvenile snakehead (*Channa argus*). *Comp. Biochem. Physiol. A* **161**, 401-405.
Weibel, E. R., Taylor, C. R. and Hoppeler, H. (1991). The concept of symmorphosis: a testable hypothesis of structure-function relationship. *Proc. Natl. Acad. Sci. USA* **88**, 10357-10361.
Wells, P. R. and Pinder, A. W. (1996a). The respiratory development of Atlantic salmon. I. Morphometry of gills, yolk sac and body surface. *J. Exp. Biol.* **199**, 2725-2736.
Wells, P. R. and Pinder, A. W. (1996b). The respiratory development of Atlantic salmon. II. Partitioning of oxygen uptake among gills, yolk sac and body surfaces. *J. Exp. Biol.* **199**, 2737-2744.
West, G. B., Brown, J. H. and Enquist, B. J. (1997). A general model for the origin of allometric scaling laws in biology. *Science* **276**, 122-126.
Xie, X. J. and Sun, R. Y. (1990). The bioenergetics of the southern catfish (*Silurus meridionalis* Chen): resting metabolic rate as a function of body weight and temperature. *Physiol. Zool.* **63**, 1181-1195.
Zhang, Y., Huang, Q., Liu, S., He, D., Wei, G. and Luo, Y. (2014). Intraspecific mass scaling of metabolic rates in grass carp (*Ctenopharyngodon idellus*). *J. Comp. Physiol. B* **184**, 347-354.

Script 1. SOURCE CODE FOR PROC MODEL IN SAS 9.4

```
data WORK.IMPORT;
input X1  X2      Y;
datalines;

/*1 STRAIGHT LINE (NO INTERCEPT) FITTED TO RAW DATA; NORMAL, HOMOSCEDASTIC
ERROR, WITH INTERACTION */
proc model data=WORK.IMPORT method=Marquardt PRL=both;
parms b=1 c=0 d=0;
Y = b*X1 + c*X2 + d*X1*X2;
h.Y = sigma**2;
fit Y/ FIML normal white breusch=(1 X1) out = output1outpredict outresid;
run;

/*2 STRAIGHT LINE (NO INTERCEPT) FITTED TO RAW DATA; NORMAL, HOMOSCEDASTIC
ERROR, WITH NO INTERACTION */
proc model data=WORK.IMPORT method=Marquardt PRL=both;
parms b=1 c=0;
Y = b*X1 + c*X2;
h.Y = sigma**2;
fit Y/ FIML normal white breusch=(1 X1) out = output2 outpredict outresid;
run;


/*  3 STRAIGHT LINE (NO INTERCEPT) FITTED TO RAW DATA; NORMAL, HETEROSCEDASTIC
ERROR, WITH INTERACTION  */
proc model data=WORK.IMPORT method=Marquardt PRL=both;
parms b=1 c=0 d=0;
Y = b*X1 + c*X2 + d*X1*X2;
h.Y = sigma**2 * (X1**(2*alpha));
fit Y/ FIML normal white breusch=(1 X1) out = output3 outpredict outresid;
run;

/*  4 STRAIGHT LINE (NO INTERCEPT) FITTED TO RAW DATA; NORMAL, HETEROSCEDASTIC
ERROR, WITH NO INTERACTION  */
proc model data=WORK.IMPORT method=Marquardt PRL=both;
parms b=1 c=0;
Y = b*X1 + c*X2;
h.Y = sigma**2 * (X1**(2*alpha));
fit Y/ FIML normal white breusch=(1 X1) out = output4 outpredict outresid;
run;

/*  5 STRAIGHT LINE (NO INTERCEPT) FITTED TO RAW DATA; LOGNORMAL,
HETEROSCEDASTIC ERROR, WITH INTERACTION  */
proc model data=WORK.IMPORT method=Marquardt PRL=both;
parms b=1 c=0 d=0;
Y = b*X1 + c*X2 + d*X1*X2;
resid.Y = log (actual.Y/pred.Y);
fit Y/ FIML normal white breusch=(1 X1) out = output5 outpredict outresid;
run;

/*  6 STRAIGHT LINE (NO INTERCEPT) FITTED TO RAW DATA; LOGNORMAL,
HETEROSCEDASTIC ERROR, WITH NO INTERACTION  */
```

```
proc model data=WORK.IMPORT method=Marquardt PRL=both;
parms b=1 c=0;
Y = b*X1 + c*X2;
resid.Y = log (actual.Y/pred.Y);
fit Y/ FIML normal white breusch=(1 X1) out = output6 outpredict outresid;
run;

/* 7 STRAIGHT LINE (INTERCEPT) FITTED TO RAW DATA; NORMAL, HOMOSCEDASTIC ERROR,
WITH INTERACTION */
proc model data=WORK.IMPORT method=Marquardt PRL=both;
parms b=1 c=0 d=0 y0=0;
Y = b*X1 + c*X2 + d*X1*X2 + y0;
h.Y = sigma**2;
fit Y/ FIML normal white breusch=(1 X1) out = output7 outpredict outresid;
run;

/* 8 STRAIGHT LINE (INTERCEPT) FITTED TO RAW DATA; NORMAL, HOMOSCEDASTIC ERROR,
WITH NO INTERACTION */
proc model data=WORK.IMPORT method=Marquardt PRL=both;
parms b=1 c=0 y0=0;
Y = b*X1 + c*X2 + y0;
h.Y = sigma**2;
fit Y/ FIML normal white breusch=(1 X1) out = output8 outpredict outresid;
run;

/*  9 STRAIGHT LINE (INTERCEPT) FITTED TO RAW DATA; NORMAL, HETEROSCEDASTIC
ERROR, WITH INTERACTION  */
proc model data=WORK.IMPORT method=Marquardt PRL=both;
parms b=1 c=0 d=0 y0=0;
Y = b*X1 + c*X2 + d*X1*X2 + y0;
h.Y = sigma**2 * (X1**(2*alpha));
fit Y/ FIML normal white breusch=(1 X1) out = output9 outpredict outresid;
run;

/*  10 STRAIGHT LINE (INTERCEPT) FITTED TO RAW DATA; NORMAL, HETEROSCEDASTIC
ERROR, WITH NO INTERACTION  */
proc model data=WORK.IMPORT method=Marquardt PRL=both;
parms b=1 c=0 y0=0;
Y = b*X1 + c*X2 + y0;
h.Y = sigma**2 * (X1**(2*alpha));
fit Y/ FIML normal white breusch=(1 X1) out = output10 outpredict outresid;
run;

/*  11 STRAIGHT LINE (INTERCEPT) FITTED TO RAW DATA; LOGNORMAL, HETEROSCEDASTIC
ERROR, WITH INTERACTION  */
proc model data=WORK.IMPORT method=Marquardt PRL=both;
parms b=1 c=0 d=0 y0=0;
Y = b*X1 + c*X2 + d*X1*X2 + y0;
resid.Y = log (actual.Y/pred.Y);
fit Y/ FIML normal white breusch=(1 X1) out = output11 outpredict outresid;
run;
```

```
/*  12 STRAIGHT LINE (INTERCEPT) FITTED TO RAW DATA; LOGNORMAL, HETEROSCEDASTIC
ERROR, WITH NO INTERACTION  */
proc model data=WORK.IMPORT method=Marquardt PRL=both;
parms b=1 c=0 y0=0;
Y = b*X1 + c*X2 + y0;
resid.Y = log (actual.Y/pred.Y);
fit Y/ FIML normal white breusch=(1 X1) out = output12 outpredict outresid;
run;

/*  13 POWER FUNCTION  (NO INTERCEPT) FITTED TO RAW DATA; NORMAL, HOMOSCEDASTIC
ERROR, WITH INTERACTION  */
proc model data=WORK.IMPORT method=Marquardt PRL=both;
parms a=1 b=1 c=0 d=0;
Y = a * X1**(b+d*X2)*exp(c*X2);
h.Y = sigma**2;
fit Y/ FIML normal white breusch=(1 X1) out = output13 outpredict outresid;
run;

/*  14 POWER FUNCTION  (NO INTERCEPT) FITTED TO RAW DATA; NORMAL, HOMOSCEDASTIC
ERROR, WITH NO INTERACTION  */
proc model data=WORK.IMPORT method=Marquardt PRL=both;
parms a=1 b=1 c=0;
Y = a * X1**b*exp(c*X2);
h.Y = sigma**2;
fit Y/ FIML normal white breusch=(1 X1) out = output14 outpredict outresid;
run;

/*  15 POWER FUNCTION  (NO INTERCEPT) FITTED TO RAW DATA; NORMAL,
HETEROSCEDASTIC ERROR, WITH INTERACTION  */
proc model data=WORK.IMPORT method=Marquardt PRL=both;
parms a=1 b=1 c=0 d=0;
Y = a * X1**(b+d*X2)*exp(c*X2);
h.Y = sigma**2 * (X1**(2*alpha));
fit Y/ FIML normal white breusch=(1 X1) out = output15 outpredict outresid;
run;

/*  16 POWER FUNCTION  (NO INTERCEPT) FITTED TO RAW DATA; NORMAL,
HETEROSCEDASTIC ERROR, WITH NO INTERACTION  */
proc model data=WORK.IMPORT method=Marquardt PRL=both;
parms a=1 b=1 c=0;
Y = a * X1**b*exp(c*X2);
h.Y = sigma**2 * (X1**(2*alpha));
fit Y/ FIML normal white breusch=(1 X1) out = output16 outpredict outresid;
run;

/*  17 POWER FUNCTION  (NO INTERCEPT) FITTED TO RAW DATA; LOGNORMAL,
HETEROSCEDASTIC ERROR, WITH INTERACTION  */
proc model data=WORK.IMPORT method=Marquardt PRL=both;
parms a=1 b=1 c=0 d=0;
Y = a * X1**(b+d*X2)*exp(c*X2);
resid.Y = log (actual.Y/pred.Y);
fit Y/ FIML normal white breusch=(1 X1) out = output17 outpredict outresid;
run;
```

```
/*  18 POWER FUNCTION  (NO INTERCEPT) FITTED TO RAW DATA; LOGNORMAL,
HETEROSCEDASTIC ERROR, WITH NO INTERACTION  */
proc model data=WORK.IMPORT method=Marquardt PRL=both;
parms a=1 b=1 c=0;
Y = a * X1**b*exp(c*X2);
resid.Y = log (actual.Y/pred.Y);
fit Y/ FIML normal white breusch=(1 X1) out = output18 outpredict outresid;
run;

/*  19 POWER FUNCTION  (INTERCEPT) FITTED TO RAW DATA; NORMAL, HOMOSCEDASTIC
ERROR, WITH INTERACTION  */
proc model data=WORK.IMPORT method=Marquardt PRL=both;
parms a=1 b=1 c=0 d=0 y0=0;
Y = a * X1**(b+d*X2)*exp(c*X2) + y0;
h.Y = sigma**2;
fit Y/ FIML normal white breusch=(1 X1) out = output19 outpredict outresid;
run;

/*  20 POWER FUNCTION (INTERCEPT) FITTED TO RAW DATA; NORMAL, HOMOSCEDASTIC
ERROR, WITH NO INTERACTION  */
proc model data=WORK.IMPORT method=Marquardt PRL=both;
parms a=1 b=1 c=0 y0=0;
Y = a * X1**b*exp(c*X2) + y0;
h.Y = sigma**2;
fit Y/ FIML normal white breusch=(1 X1) out = output20 outpredict outresid;
run;

/*  21 POWER FUNCTION (INTERCEPT) FITTED TO RAW DATA; NORMAL, HETEROSCEDASTIC
ERROR, WITH INTERACTION  */
proc model data=WORK.IMPORT method=Marquardt PRL=both;
parms a=1 b=1 c=0 d=0 y0=0;
Y = a * X1**(b+d*X2)*exp(c*X2) + y0;
h.Y = sigma**2 * (X1**(2*alpha));
fit Y/ FIML normal white breusch=(1 X1) out = output21 outpredict outresid;
run;

/*  22 POWER FUNCTION (INTERCEPT) FITTED TO RAW DATA; NORMAL, HETEROSCEDASTIC
ERROR, WITH NO INTERACTION  */
proc model data=WORK.IMPORT method=Marquardt PRL=both;
parms a=1 b=1 c=0 y0=0;
Y = a * X1**b*exp(c*X2) + y0;
h.Y = sigma**2 * (X1**(2*alpha));
fit Y/ FIML normal white breusch=(1 X1) out = output22 outpredict outresid;
run;


/*  23 POWER FUNCTION (INTERCEPT) FITTED TO RAW DATA; LOGNORMAL,
HETEROSCEDASTIC ERROR, WITH INTERACTION */
proc model data=WORK.IMPORT method=Marquardt PRL=both;
parms a=1 b=1 c=0 d=0 y0=0;
Y = a * X1**(b+d*X2)*exp(c*X2) + y0;
resid.Y = log (actual.Y/pred.Y);
```

```
fit Y/ FIML normal white breusch=(1 X1) out = output23 outpredict outresid;
run;

/*  24 POWER FUNCTION (INTERCEPT) FITTED TO RAW DATA; LOGNORMAL,
HETEROSCEDASTIC ERROR, WITH NO INTERACTION */
proc model data=WORK.IMPORT method=Marquardt PRL=both;
parms a=1 b=1 c=0 y0=0;
Y = a * X1**(b)*exp(c*X2) + y0;
resid.Y = log (actual.Y/pred.Y);
fit Y/ FIML normal white breusch=(1 X1) out = output24 outpredict outresid;
run;

/*  IF NONLINEAR MODELS FAIL TO CONVERGE, TRY INCREASING THE NUMBER
OF ITERATIONS AND/OR RELAXING THE CONVERGENCE CRITERION, e.g.,
   iter=200  converge=0.01   AND TRY CHANGING START VALUES FOR THE
PARAMETERS. IF THE VALUE FOR c WAS NOT SIGNIFICANT, THEN THE
PARAMETER  c WAS DROPPED FROM THE MODEL AND THE MODEL WITH NO X2
TERM WAS USED TO ANALYSIS. */
```

Table S1. Statistical models fitted to untransformed data for scalings.

Click here to Download Table S1